Inorg. Chem. **2009**, *48*, 1606−1612

Mixed-Valent $\{Mn_{14}\}$ Aggregate Encapsulated by the Inorganic Polyoxometalate Shell: $[Mn^{III}_{13}Mn^{II}O_{12}(PO_4)_4(PW_9O_{34})_4]^{31-}$

Qiong Wu,[†] Yang-Guang Li,*[,†] Yong-Hui Wang,[†] En-Bo Wang,*[,†] Zhi-Ming Zhang,[†] and Rodolphe Clérac*[,‡,§]

Key Laboratory of Polyoxometalate Science of Ministry of Education, Faculty of Chemistry, Northeast Normal University, Changchun, Jilin 130024, People's Republic of China, CNRS, UPR 8641, Centre de Recherche Paul Pascal (CRPP), Equipe "Matériaux Moléculaires Magnétiques", 115 avenue du Dr. Albert Schweitzer, Pessac F-33600, France, and Université de Bordeaux, UPR 8641, Pessac F-33600, France

Received October 22, 2008

The reaction of $[Mn_{12}(CH_3COO)_{16}(H_2O)_4O_{12}]\cdot 2CH_3COOH\cdot 4H_2O$, $Na_8[HPW_9O_{34}]\cdot 24H_2O$, K_2HPO_4, and ethylenediamine hydrochloride in an aqueous solution leads to the isolation of a new polyoxometalate-based mixed-valent manganese aggregate, $K_{14}Na_{17}[(Mn^{III}_{13}Mn^{II}O_{12}(PO_4)_4(PW_9O_{34})_4]\cdot\sim 56H_2O$ (**1**). Single-crystal X-ray diffraction indicates that the polyoxoanion of **1** exhibits a mixed-valent $[Mn^{III}_{13}Mn^{II}(\mu_2\text{-}O)_6(\mu_3\text{-}O)_6(\mu_4\text{-}PO_4)_2(\mu_5\text{-}PO_4)_2]^{5+}$ complex encapsulated by four $[B\text{-}\alpha\text{-}PW_9O_{34}]^{9-}$ trivacant Keggin-type moieties [crystal data for **1**: monoclinic, *C*2/*c* (No. 15), $a = 36.341(7)$ Å, $b = 18.325(4)$ Å, $c = 36.668(7)$ Å, $\beta = 119.24(3)°$, $V = 21308(7)$ Å^3, $Z = 4$]. In a magnetic point of view, all of these paramagnetic manganese aggregates in **1** are well wrapped into the diamagnetic inorganic shells. Variable-temperature, solid-state, direct-current susceptibility measurements show that compound **1** exhibits strong antiferromagnetic interactions inside the $[Mn_{14}]$ core.

Introduction

The extensive interest in the polynuclear transition-metal (TM) complexes is due to not only their aesthetically pleasing structures but also their potential applications in nanomagnets, catalysis, and optical materials.[1] During the assembly of polynuclear TM complexes, an extensively employed strategy is the use of various multidentate O- or N-donor organic ligands to coordinate, bridge, and bind more metal centers into aggregates with abundant kinds of nuclearities.[2−7] Furthermore, these organic ligands generally act as one kind of diamagnetic organic shell that can well encapsulate the inner paramagnetic TM cores (as shown in Scheme 1).[8] In comparison, polyoxometalates (POMs), as a unique

* To whom correspondence should be addressed. E-mail: liyg658@nenu.edu.cn (Y.-G.L.), wangenbo@public.cc.jl.cn (E.-B.W.), clerac@crpp-bordeaux.cnrs.fr (R.C.).
† Northeast Normal University.
‡ Centre de Recherche Paul Pascal (CRPP).
§ Université de Bordeaux.

(1) (a) Ford, P. C.; Cariati, E.; Bourassa, J. *Chem. Rev.* **1999**, *99*, 3625. (b) Müller, A.; Shah, S. Q. N.; Bögge, H. *Nature* **1999**, *397*, 48. (c) Wassermann, K.; Dickman, M. H.; Pope, M. T. *Angew. Chem., Int. Ed. Engl.* **1997**, *36*, 1445. (d) Tasiopoulos, A. J.; Vinslava, A.; Wernsdorfer, W.; Abboud, K. A.; Christou, G. *Angew. Chem., Int. Ed.* **2004**, *43*, 2117. (e) Liu, T.; Zhang, Y.-J.; Wang, Z.-M.; Gao, S. *J. Am. Chem. Soc.* **2008**, *130*, 10500. (f) Dearden, A. L.; Parsons, S.; Winpenny, R. E. P. *Angew. Chem., Int. Ed.* **2001**, *40*, 151. (g) Murugesu, M.; Clérac, R.; Anson, C. E.; Powell, A. K. *Inorg. Chem.* **2004**, *43*, 7269. (h) Fang, X. K.; Anderson, T. M.; Hill, C. L. *Angew. Chem., Int. Ed.* **2005**, *44*, 3540. (i) Hu, A. G.; Yee, G. T.; Lin, W. B. *J. Am. Chem. Soc.* **2005**, *127*, 12486. (j) Wu, C. D.; Lin, W. B. *Inorg. Chem.* **2005**, *44*, 1178. (k) Li, G.; Yu, W. B.; Cui, Y. *J. Am. Chem. Soc.* **2008**, *130*, 4582.

(2) (a) Ako, A. M.; Hewitt, I. J.; Mereacre, V.; Clérac, R.; Wernsdorfer, W.; Anson, C. E.; Powell, A. K. *Angew. Chem., Int. Ed.* **2006**, *45*, 4926. (b) Li, Y.; Wernsdorfer, W.; Clérac, R.; Hewitt, I. J.; Anson, C. E.; Powell, A. K. *Inorg. Chem.* **2006**, *45*, 2376. (c) Scott, R. T. W.; Parsons, S.; Murugesu, M.; Wernsdorfer, W.; Christou, G.; Brechin, E. K. *Angew. Chem., Int. Ed.* **2005**, *44*, 6540. (d) Soler, M.; Wernsdorfer, W.; Folting, K.; Pink, M.; Christou, G. *J. Am. Chem. Soc.* **2004**, *126*, 2156. (e) Zaleski, C. M.; Depperman, E. C.; Dendrinou-Samara, C.; Alexiou, M.; Kampf, J. W.; Kessissoglou, D. P.; Kirk, M. L.; Pecoraro, V. L. *J. Am. Chem. Soc.* **2005**, *127*, 1286. (f) Miyasaka, H.; Clérac, R.; Wernsdorfer, W.; Lecren, L.; Bonhomme, C.; Sugiura, K.; Yamashita, M. *Angew. Chem., Int. Ed.* **2004**, *43*, 2801.

(3) (a) Powell, A. K.; Heath, S. L.; Gatteschi, D.; Pardi, L.; Sessoli, R.; Spina, G.; Giallo, F. D.; Pieralli, F. *J. Am. Chem. Soc.* **1995**, *117*, 2491. (b) Sangregorio, C.; Ohm, T.; Paulsen, C.; Sessoli, R.; Gatteschi, D. *Phys. Rev. Lett.* **1997**, *78*, 4645. (c) Oshio, H.; Hoshino, N.; Ito, T. *J. Am. Chem. Soc.* **2000**, *122*, 12602. (d) Barra, A. L.; Caneschi, A.; Cornia, A.; Fabrizide Biani, F.; Gatteschi, D.; Sangregorio, C.; Sessoli, R.; Sorace, L. *J. Am. Chem. Soc.* **1999**, *121*, 5302.

(4) (a) Brechin, E. K.; Coxall, R. A.; Parkin, A.; Parsons, S.; Tasker, P. A.; Winpenny, R. E. P. *Angew. Chem., Int. Ed.* **2001**, *40*, 700. (b) Murrie, M.; Teat, S. J.; Stoeckli-Evans, H.; Güdel, H. U. *Angew. Chem., Int. Ed.* **2003**, *42*, 4653. (c) Yang, E.-C.; Hendrickson, D. N.; Wernsdorfer, W.; Nakano, M.; Zakharov, L. N.; Sommer, R. D.; Rheingold, A. L.; Ledezma-Gairaud, M.; Christou, G. *J. Appl. Phys.* **2002**, *91*, 7382.

10.1021/ic802023h CCC: $40.75
Published on Web 01/22/2009

Scheme 1. Schematic View of the Simplified Model of the Polynuclear TM Complexes[a]

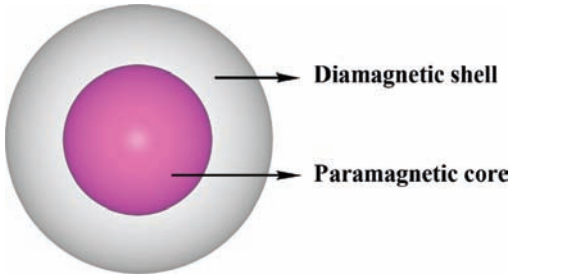

[a] In this structural model, the diamagnetic shell can be multidentate organic ligands or inorganic POM ligands.

class of metal oxide complexes with versatile structural topologies and nucleophilic oxygen-enriched surfaces,[9] can act as excellent inorganic multidentate O-donor ligands to assemble polynuclear TM aggregates.[10,11] Recently, a series of lacunary POM moieties have been used to construct a handful of significantly large paramagnetic TM complexes, such as $[K_8\square\{V_6O_{12}(H_2O)_2\}_2\{P_8W_{48}O_{184}\}]^{24-}$,[11a] $[Mn_6O_4(H_2O)_4(XW_9O_{34})_2]^{12-}$,[11b] $[(MnCl)_6(\alpha\text{-}XW_9O_{33})_2]^{12-}$,[11c] $[Fe^{III}_{12}Fe^{II}(OH)_{12}(PO_4)_4(PW_9O_{34})_4]^{22-}$,[11d] $[K\square Fe_{12}(OH)_{18}(P_2W_{15}O_{56})_4]^{29-}$,[11e] $[Fe_{27}P_8W_{49}O_{248}H_{55}]^{26-}$,[11f] $[Co_6(H_2O)_{30}Co_9Cl_2(OH)_3(H_2O)_9(SiW_8O_{31})_3]^{5-}$,[11g] $[M_9(OH)_3(H_2O)_6(HPO_4)_2(PW_9O_{34})3]^{16-}$ ($M = Ni^{2+}/Co^{2+}$),[11h] $[Cu_{14}(OH)_{12}X(SiW_9O_{34})_2(SiW_9O_{33}(OH))_2]^{23-}$ ($X = Cl^-/Br^-$),[11i] $[Cu_{20}Cl(OH)_{24}(H_2O)_{12}(P_8W_{48}O_{184})]^{25-}$,[11j] and $[Cu_{20}(N_3)_6(OH)_{18}P_8W_{48}O_{184}]^{24-}$.[11k] In these compounds, the paramagnetic complexes are semiencapsulated or fully encapsulated by the inorganic POM shells. Because spin carriers in these types of compounds can be well separated by the diamagnetic POM ligands, one goal in this research subfield is appearing to explore the magnetically interesting POM-based TM complexes, especially the single-molecule magnets (SMMs) that can be used for high-density information storage and quantum computation.[12] The special properties of SMMs stem from the combination of a large spin ground state (S) and uniaxial-type anisotropy (D; considering the Hamiltonian of anisotropy $H = DS_{z^2}$), which create a superparamagnetic-like behavior.[12] In this area, most of the interest for SMMs is focused on polynuclear Mn^{III} clusters because these complexes include the necessary ingredients of SMMs and especially a large uniaxial anisotropy arising from the presence of Jahn−Teller distorted Mn^{III} ions.[2,12] Therefore, the Mn^{III} metal ion appears to be a good choice for preparing POM-based SMMs. Nevertheless, despite the enormous success on POM-based TM complexes, little progress has been gained in the synthesis of large POMs including Mn^{III} aggregates.[13] The only successful example is $[Mn^{III}_2Mn^{II}_4O_4(H_2O)_4(XW_9O_{34})_2]^{12-}$, exhibiting the first POM-based Mn complex with SMM behavior.[11b] During the synthesis of POM-based Mn^{III}-containing complexes, the main difficulty is to keep the Mn^{III} ions stable in an aqueous POM-containing reaction system because Mn^{III} ions tend to convert into Mn^{II} and Mn^{IV}. Until now, there are two routes to prepare the POM-based Mn^{III} complexes. The first one is the use of strong oxidation agents to react with the POM-based Mn^{II}-containing compounds in order to oxidize the Mn^{II} centers into Mn^{III} centers. However, there are only a few available POM-based Mn^{II} complex systems to carry

(5) Cadiou, C.; Murrie, M.; Paulsen, C.; Villar, V.; Wernsdorfer, W.; Winpenny, R. E. P. *Chem. Commun.* **2001**, 2666.
(6) Murugesu, M.; Anson, C. E.; Powell, A. K. *Chem. Commun.* **2002**, 1054.
(7) (a) Castro, S. L.; Sun, Z.; Grant, C. M.; Bollinger, J. C.; Hendrickson, D. N.; Christou, G. *J. Am. Chem. Soc.* **1998**, *120*, 2365. (b) Hegetschweiler, K.; Morgenstern, B.; Zubieta, J.; Hagrman, P. J.; Lima, N.; Sessoli, R.; Totti, F. *Angew. Chem., Int. Ed.* **2004**, *43*, 3436. (c) Karet, G. B.; Sun, Z.; Heinrich, D. D.; McCusker, J. K.; Folting, K.; Streib, W. E.; Huffman, J. C.; Hendrickson, D. N.; Christou, G. *Inorg. Chem.* **1996**, *35*, 6450.
(8) Schmitt, W.; Murugesu, M.; Goodwin, J. C.; Hill, J. P.; Mandel, A.; Bhalla, R.; Anson, C. E.; Heath, S. L.; Powell, A. K. *Polyhedron* **2001**, *20*, 1687.
(9) (a) Pope, M. T. *Heteropoly and Isopoly Oxometalates*; Springer: Berlin, 1983. (b) Pope, M. T.; Müller, A. *Polyoxometalates: From Platonic Solids to Anti-Retroviral Activity*; Kluwer: Dordrecht, The Netherlands, 1993. (c) Hill, C. L., Ed. Special Issue on Polyoxometalates. *Chem. Rev.* **1998**, *98*, 1. (d) Pope, M. T., Müller, A., Eds. *Polyoxometalate Chemistry: From Topology via Self-Assembly to Applications*; Kluwer: Dordrecht, The Netherlands, 2001. (e) Yamase, T.; Pope, M. T., Eds. *Polyoxometalate Chemistry for Nano-Composite Design*; Kluwer: Dordrecht, The Netherlands, 2002. (f) Long, D. L.; Burkholder, E.; Cronin, L. *Chem. Soc. Rev.* **2007**, *36*, 105.
(10) (a) Zhang, Z.; Qi, Y.; Qin, C.; Li, Y.; Wang, E.; Wang, X.; Su, Z.; Xu, L. *Inorg. Chem.* **2007**, *46*, 8162. (b) Zhang, Z.; Li, Y.; Wang, E.; Wang, X.; Qin, C.; An, H. *Inorg. Chem.* **2006**, *45*, 4313. (c) Zhang, Z.; Wang, E.; Qi, Y.; Li, Y.; Mao, B.; Su, Z. *Cryst. Growth Des.* **2007**, *7*, 1305. (d) Chen, W. L.; Li, Y. G.; Wang, Y. H.; Wang, E. B.; Su, Z. M. *Dalton Trans.* **2007**, *38*, 4293. (e) Chen, W. L.; Li, Y. G.; Wang, Y. H.; Wang, E. B.; Zhang, Z. M. *Dalton Trans.* **2008**, *7*, 865.
(11) (a) Müller, A.; Pope, M. T.; Todea, A. M.; Bögge, H.; Van Slageren, J.; Dressel, M.; Gouzerh, P.; Thouvenot, R.; Tsukerblat, B.; Bell, A. *Angew. Chem., Int. Ed.* **2007**, *46*, 4477. (b) Ritchie, C.; Ferguson, A.; Nojiri, H.; Miras, H. N.; Song, Y. F.; Long, D. L.; Burkholder, E.; Murrie, M.; K'gerler, P.; Brechin, E. K.; Cronin, L. *Angew. Chem., Int. Ed.* **, 2008**, *47*, 5609. (c) Yamase, T.; Fukaya, K.; Nojiri, H.; Ohshima, Y. *Inorg. Chem.* **2006**, *45*, 7698. (d) Zhao, J. W.; Zhang, J.; Zheng, S. T.; Yang, G. Y. *Inorg. Chem.* **2007**, *46*, 10944. (e) Pradeep, C. P.; Long, D. L.; Kögerlerb, P.; Cronin, L. *Chem. Commun.* **2007**, 4254. (f) Godin, B.; Chen, Y. G.; Vaissermann, J.; Ruhlmann, L.; Verdaguer, M.; Gouzerh, P. *Angew. Chem., Int. Ed.* **2005**, *44*, 3072. (g) Bassil, B. S.; Nellutla, S.; Kortz, U.; Stowe, A. C.; van Tol, J.; Dalal, N. S.; Keita, B.; Nadjo, L. *Inorg. Chem.* **2005**, *44*, 2659. (h) Clemente-Juan, J. M.; Coronado, E.; Galan-Mascaros, J. R.; Gomez-Garcia, C. J. *Inorg. Chem.* **1999**, *38*, 55. (i) Mialane, P.; Dolbecq, A.; Marrot, J.; Riviere, E.; Secheresse, F. *Angew. Chem., Int. Ed.* **2003**, *42*, 3523. (j) Mal, S. S.; Kortz, U. *Angew. Chem., Int. Ed.* **2005**, *44*, 3777. (k) Pichon, C.; Mialane, P.; Dolbecq, A.; Marrot, J.; Rivière, E.; Keita, B.; Nadjo, L.; Secheresse, F. *Inorg. Chem.* **2007**, *46*, 5292.
(12) (a) Sessoli, R.; Ysai, H.-L.; Schake, A. R.; Wang, S.; Vincent, J. B.; Folting, K.; Gatteschi, D.; Christou, G.; Hendrickson, D. N. *J. Am. Chem. Soc.* **1993**, *115*, 1804. (b) Sessoli, R.; Gatteschi, D.; Caneschi, A.; Novak, M. A. *Nature* **1993**, *356*, 141. (c) Christou, G.; Gatteschi, D.; Hendrickson, D. N.; Sessoli, R. *MRS Bull.* **2000**, *25*, 66. (d) Lis, T. *Acta Crystallogr., Sect. B* **1980**, *36*, 2042. (e) Sessoli, R.; Tsai, H. L.; Schake, A. R.; Wang, S.; Vincent, J. B.; Folting, K.; Gatteschi, D.; Christou, G.; Hendrickson, D. N. *J. Am. Chem. Soc.* **1993**, *115*, 1804.
(13) (a) Zhang, X. Y.; Pope, M. T.; Chance, M. R.; Jameson, G. B. *Polyhedron* **1995**, *14*, 1381. (b) Zhang, X. Y.; O'Connor, C. J.; Jameson, G. B.; Pope, M. T. *Inorg. Chem.* **1996**, *35*, 30. (c) Liu, J. F.; Ortega, F.; Pope, M. T. *J. Chem. Soc., Dalton Trans.* **1992**, 1901. (d) Zhang, X. Y.; O'Connor, C. J.; Jameson, G. B.; Pope, M. T. *Polyhedron* **1996**, *15*, 917. (e) Gómez-García, C. J.; Coronado, E.; Gómez-Romero, P.; Casan-Pastor, N. *Inorg. Chem.* **1993**, *32*, 3378. (f) Gómez-García, C. J.; Borras-Almenar, J. J.; Coronado, E.; Ouahab, L. *Inorg. Chem.* **1994**, *33*, 4016. (g) Zhang, Z. M.; Wang, E. B.; Chen, W. L.; Tan, H. Q. *Aust. J. Chem.* **2007**, *60*, 284. (h) Mialane, P.; Duboc, C.; Marrot, J.; Rivière, E.; Dolbecq, A.; Secheresse, F. *Chem.—Eur. J.* **2006**, *12*, 1950. (i) Fang, X.; Kögerler, P. *Chem. Commun.* **2008**, 3396. (j) Ritchie, C.; Burkholder, E. M.; Long, D. L.; Adam, D.; Kögerler, P.; Cronin, L. *Chem. Commun.* **2007**, 468.
(14) Massart, R.; Contant, R.; Fruchart, J. M.; Ciabrini, J. P.; Fournier, M. *Inorg. Chem.* **1977**, *16*, 2916.

out such a preparation.[13a−g] The other way is the introduction of various organic amines into the reaction systems containing POM ligands and Mn^{II} ions.[11b,13h] During the reaction, the solution should be exposed to air so as to oxidize Mn^{II} ions into Mn^{III}. The disadvantage of such an approach is that the reaction process is difficult to control because precipitation and decomposition of POM ligands often happen during the preparation. An alternative synthetic route is to start from the preformed Mn^{III} complexes and react them with various POM ligands. This type of synthetic strategy has been extensively employed in the synthesis of organic-ligand-based manganese complexes;[2] however, it is rarely used for the synthesis of POM-based manganese complexes.[13i] Because most of the well-known manganese complexes are isolated from basic and organic media that are usually not adapted for the acidic and water-soluble POM ligands, the choice of a suitable Mn^{III} complex precursor and POM ligands becomes critical in this approach.

On the basis of aforementioned considerations, we start investigating the reactions between the trivacant Keggin-type polyoxoanions $[PW_9O_{34}]^{9-}$ and the well-known SMM $\{Mn_{12}\}$ complex,[12] which are obtained from the acidic aqueous solution in order to explore this new route of preparing POM-based Mn^{III}-containing complexes. Herein, we report a new $\{Mn_{14}\}$ aggregate based on the trivacant Keggin-type POMs, $K_{14}Na_{17}[(Mn^{III}{}_{13}Mn^{II}O_{12}(PO_4)_4(PW_9O_{34})_4]\cdot\sim 56H_2O$ (**1**). To the best of our knowledge, compound **1** represents the currently largest manganese aggregates based on the inorganic POM ligands.

Experimental Section

Materials and Methods. All chemicals were commercially purchased and used without further purification. The starting materials of $[Mn_{12}(CH_3COO)_{16}(H_2O)_4O_{12}]\cdot 2CH_3COOH\cdot 4H_2O$[12d] and β-$Na_8[HPW_9O_{34}]\cdot 24H_2O$[14] were synthesized according to the literature and characterized by IR spectra. Elemental analyses of P, W, Mn, K, and Na were analyzed on a PLASMA-SPEC (I) inductively coupled plasma atomic emission spectrometer. The IR spectrum was recorded in the range 400−4000 cm^{-1} on an Alpha Centaurt FTIR spectrophotometer using KBr pellets. An UV−vis absorption spectrum was obtained using a PC 752 UV−vis spectrophotometer. Thermogravimetric (TG) analyses were performed on a Perkin-Elmer TGA7 instrument in flowing N_2 with a heating rate of 10 °C·min^{-1}. X-ray photoelectron spectroscopy (XPS) analyses were performed on a VG ESCALABMKII spectrometer with an Mg Kα (1253.6 eV) achromatic X-ray source. The vacuum inside the analysis chamber was maintained at 6.2×10^{-6} Pa during the analysis. The magnetic susceptibility measurements were obtained with the use of a Quantum Design SQUID magnetometer MPMS-XL housed at the Centre de Recherche Paul Pascal. This magnetometer works between 1.8 and 400 K for direct-current (dc) applied fields ranging from −7 to +7 T. Measurements were performed on a polycrystalline sample of 17.77 mg. Alternating-current (ac) susceptibility measurements have been measured with an oscillating ac field of 3 Oe and ac frequencies ranging from 1 to 1500 Hz. The magnetic data were corrected for the sample holder and diamagnetic contributions.[15] M vs H measurements were performed at 100 K to check for the presence of ferromagnetic impurities, which were found to be absent.

Synthesis of 1. β-$Na_8[HPW_9O_{34}]\cdot 24H_2O$ (2.85 g, 1.0 mmol) and K_2HPO_4 (0.174 g, 1.0 mmol) were dissolved in 40 mL of distilled water with vigorous stirring for 10 min. Then, a small amount of insoluble substance was removed by filtration. To the above solution was added dropwise within 10 min 20 mL of aqueous solution containing the freshly prepared $[Mn_{12}(CH_3COO)_{16}(H_2O)_4O_{12}]\cdot 2CH_3COOH\cdot 4H_2O$ (0.61 g, 0.3 mmol). The mixture was stirred for 1 h at room temperature. During this time, ethylenediamine hydrochloride (0.06 g, 0.5 mmol) was slowly added. The resulting reaction mixture was further stirred for another 30 min at 40 °C and then cooled to the room temperature. After filtration, the dark-brown filtrate was slowly evaporated at room temperature. The light-pink platelike crystalline byproduct of **2** was quickly isolated overnight and confirmed as a sandwich-type POM[16] (yield 8.5% based on W). Then, the solution was filtered again, sealed by parafilm with a few of tiny pores, and very slowly evaporated at room temperature. After 4 weeks, dark-brown blocklike crystalline products of **1** were obtained (yield 24.6% based on W). Anal. Calcd for $H_{112}O_{220}P_8W_{36}Mn_{14}K_{14}Na_{17}$ (**1**): P, 2.03; W, 54.22; Mn, 6.30; K, 4.48; Na, 3.20. Found: P, 1.93; W, 54.56; Mn, 6.59; K, 4.21; Na, 3.34. IR (KBr disk, cm^{-1}): 3520 (br), 1620 (s), 1095 (s), 970 (s), 873 (s), 732 (s) and 615 (s). TG analysis indicates that there are about 56 lattice water molecules in the compound **1** (see the Supporting Information).

X-ray Crystallography. The crystallographic data were collected at 150 K on the Rigaku R-axis Rapid IP diffractometer using graphite monochromatic Mo Kα radiation (λ = 0.710 73 Å) and IP techniques. A multiscan absorption correction was applied. The crystal data of **1** was solved by direct methods and refined by a full-matrix least-squares method on F^2 using the *SHELXTL-97* crystallographic software package.[17] During the refinement, it was found that the Mn1 and Mn2 positions in the polyoxoanion were just half-occupied considering that their thermal parameters (U_{eq}) should be close to those of other manganese centers. On the basis of this refinement, there should be two possible $\{Mn_{14}\}$ core arrangements in the polyoxoanion of **1** (as shown in Figure S2 in the Supporting Information). The polyoxoanion and partial K^+ and Na^+ cations were anisotropically refined, while the rest of the cations and all of the solvent water molecules were just refined isotropically because of their unusual anisotropic thermal parameters and obvious disorder problems. H atoms on lattice water molecules cannot be found from the residual peaks and were directly included in the final molecular formula. It is noteworthy that only 13 Na^+ cations and 35 water molecules can be found from the difference Fourier maps. The rest, four Na^+ and another 21 water molecules, were confirmed by modeling the data with the *SQUEEZE* program[18] together with elemental and TG analyses. The detailed crystal data and structure refinement for **1** are given in Table 1. Selected bond lengths and angles of **1** are listed in Table 2, respectively. CSD reference number: 419903 for **1**.

(15) Boudreaux, E. A., Mulay, L. N., Eds. *Theory and Applications of Molecular Paramagnetism*; John Wiley & Sons: New York, 1976.

(16) The byproduct of compound **2** is $K_{11}Na_{10}[MnO_3(PW_7O_{28})_2]\cdot 26H_2O$. Crystal data for **2**: triclinic, $P\bar{1}$ (No. 2), a = 11.833(2) Å, b = 14.087(3) Å, c = 23.003(5) Å, α = 74.58(3)°, β = 84.79(3)°, γ = 84.79(3)°, Z = 2. The polyoxoanion structure of **2** is shown in Figure S8 in the Supporting Information.

(17) (a) Sheldrick, G. M. *SHELXL97, Program for Crystal Structure Refinement*; University of Göttingen: Göttingen, Germany, 1997. (b) Sheldrick, G. M. *SHELXS97, Program for Crystal Structure Solution*; University of Göttingen: Göttingen, Germany, 1997.

(18) Spek, A. L. *PLATON, A Multipurpose Crystallographic Tool*; Utrecht University: Utrecht, The Netherlands, 1998.

Table 1. Crystal Data and Structure Refinement for **1**

empirical formula	$H_{112}O_{220}P_8W_{36}Mn_{14}K_{14}Na_{17}$
M	12 206.65
λ/Å	0.710 73
T/K	150(2)
cryst dimens/mm	0.26 × 0.24 × 0.22
cryst syst	Monoclinic
space group	$C2/c$
a/Å	36.341(7)
b/Å	18.325(4)
c/Å	36.668(7)
β/deg	119.24(3)
V/Å^3	21308(7)
Z	4
D_c/Mg·m^{-3}	3.805
μ/mm^{-1}	20.632
F(000)	21836
θ range/deg	2.99−25.00
reflns collected/unique	69 027/18 328
R_{int}	0.1243
data/restraints/param	18 328/102/1197
R1 [$I > 2\sigma(I)$][a]	0.0500
wR2 (all data)[b]	0.0945
GOF on F^2	0.941
$\Delta\rho_{max,min}$/e·Å^{-3}	4.289, −1.628

[a] $R1 = \sum||F_o| - |F_c||/|F_o|$. [b] $wR2 = \sum[w(F_o^2 - F_c^2)^2]/\sum[w(F_o^2)^2]^{1/2}$.

Table 2. Selected Bond Lengths of Mn−O in **1**[a]

Mn1−O24	2.024(15)	Mn2−O30	1.965(14)
Mn1−O25	2.028(17)	Mn2−O76	2.027(16)
Mn1−O36	2.059(13)	Mn2−O76A	2.044(12)
Mn1−O62A	2.076(12)	Mn2−O2	2.078(17)
Mn1−O62	2.085(15)	Mn2−O5	2.142(14)
Mn1−O76	2.339(14)	Mn2−O62	2.338(14)
Mn3−O25	1.955(14)	Mn4−O39	1.990(16)
Mn3−O24	1.973(14)	Mn4−O49	1.991(16)
Mn3−O38	1.994(14)	Mn4−O5	1.999(16)
Mn3−O31	1.996(15)	Mn4−O2	2.011(14)
Mn3−O22A	2.090(13)	Mn4−O4A	2.078(13)
Mn3−O32	2.337(11)	Mn4−O27	2.313(12)
Mn5−O36	1.944(13)	Mn6−O36	1.954(14)
Mn5−O24	1.955(11)	Mn6−O25	1.997(12)
Mn5−O44	1.958(15)	Mn6−O16	1.997(15)
Mn5−O19	1.993(12)	Mn6−O53	2.011(12)
Mn5−O10	2.110(15)	Mn6−O23	2.041(14)
Mn5−O32	2.275(14)	Mn6−O32	2.289(13)
Mn7−O2	1.935(13)	Mn8−O5	1.886(13)
Mn7−O21	1.952(12)	Mn8−O3	1.969(15)
Mn7−O30	1.973(15)	Mn8−O30	1.988(15)
Mn7−O12	1.991(14)	Mn8−O33	1.988(13)
Mn7−O6	2.066(14)	Mn8−O26	2.112(14)
Mn7−O27	2.298(13)	Mn8−O27	2.334(14)

[a] Symmetry transformations used to generate equivalent atoms: A, $-x$, y, $-z + {}^3/_2$.

Results and Discussion

Synthesis. The design and synthesis of novel polynuclear manganese aggregates from the reactions between preformed manganese complexes and various organic N- and O-donor ligands have been widely employed;[2] however, such a synthetic route has been rarely used in the preparation of POM-based manganese aggregates.[13] It is worth mentioning that most of the polynuclear manganese precursors are obtained from the organic solution with relatively high pH values. In such conditions, most of the POM ligands are either nonsoluble or decomposed; thus, the effective assembly between manganese complexes and POMs does not happen. To use such a synthetic strategy, it is thus very important to choose suitable manganese complexes that can be isolated from the acidic aqueous solution. Interestingly, the well-known SMM $\{Mn_{12}\}$ complex $[Mn_{12}(CH_3COO)_{16}(H_2O)_4O_{12}]\cdot 2CH_3COOH\cdot 4H_2O$ is usually isolated from the water−acetic acid solution. Therefore, this complex represents one of the most suitable manganese precursors to react with the lacunary POM ligands. During the preparation of compound **1** with $\{Mn_{12}\}$ complexes and trivacant $\{PW_9\}$ POM ligands, three important factors should be emphasized. First of all, the use of K_2HPO_4 played important roles for the preparation of compound **1**.[13j] In the initial synthesis, no K_2HPO_4 was introduced into the reaction system and only a few of brown block crystals were isolated from the filtrate in 2 months with poor crystalline quality. Nevertheless, the initial single-crystal X-ray diffraction data suggested that the crystalline sample could contain a new type of polyoxoanion, $[(Mn^{III}_{13}Mn^{II}O_{12}(PO_4)_4(PW_9O_{34})_4]^{31-}$. In this polyoxoanion, the $[B\text{-}\alpha\text{-}PW_9O_{34}]^{9-}$ moieties were transferred from the β-$[HPW_9O_{34}]^{8-}$ precursors.[14] The extra $[PO_4]^{3-}$ units might come from the impurities of β-$Na_8[HPW_9O_{34}]\cdot 24H_2O$ precursors. Thus, K_2HPO_4 was introduced to improve the synthetic method. The final yield of **1** was increased and the quality of the single crystals was also improved because the K^+ cations were crystallized into the final compounds. Second, the filtered solution should be well sealed by parafilm with a few holes and kept undisturbed for very slow evaporation at room temperature. Otherwise, a lot of light-pink platelike crystalline byproduct of compound **2** was quickly isolated from the filtrate overnight and then a few brown blocklike crystals of **1** mixed with compound **2** were obtained after 3 weeks. Furthermore, even the filtrate was well sealed, a small amount of the crystalline byproduct of **2** can also be isolated from the solution after 1 day. However, when the initial byproduct was filtered, pure-brown blocklike crystals of **1** were isolated from the filtrate after 1 month of very slow evaporation. Hence, it was hypothesized that compound **2** was the kinetic product while compound **1** should be a thermodynamically stable product. Third, the use of ethylenediamine hydrochloride was also necessary in order to isolate **1**. Without it, no crystalline compound can be isolated from the reaction system, although ethylenediamine hydrochloride was not crystallized into the final molecular system. During the preparation, ethylenediamine hydrochloride might play the role of decomposing the $\{Mn_{12}\}$ complexes into smaller moieties and partially reducing the Mn^{IV} ions into Mn^{III} or Mn^{II} ions.

Crystal Description. Single-crystal X-ray diffraction analysis reveals that the polyoxoanion of **1** is composed of two $\{Mn_4\}$-substituted Keggin units, $[Mn_4O_3(B\text{-}\alpha\text{-}PW_9O_{34})]^{4-/3-}$, and two $\{Mn_3\}$-substituted Keggin fragments, $[Mn_3O_3(B\text{-}\alpha\text{-}PW_9O_{34})]^{6-}$. These four moieties are connected by four $\{PO_4\}$ linkers to form a large tetrameric aggregate (see Figures 1 and S1 in the Supporting Information). In the polyoxoanion, all of the lacunary Keggin fragments $[PW_9O_{34}]^{9-}$ (abbreviation $\{PW_9\}$) exhibit the typical trivacant B-α-Keggin-type structure. Such a structural feature can be viewed as a mother α-Keggin unit that lost three edge-sharing $\{WO_6\}$ octahedra (as shown in Scheme S1 in the Supporting Information). In these fragments, all P atoms exhibit a tetracoordination environment and all W centers display the octahedral

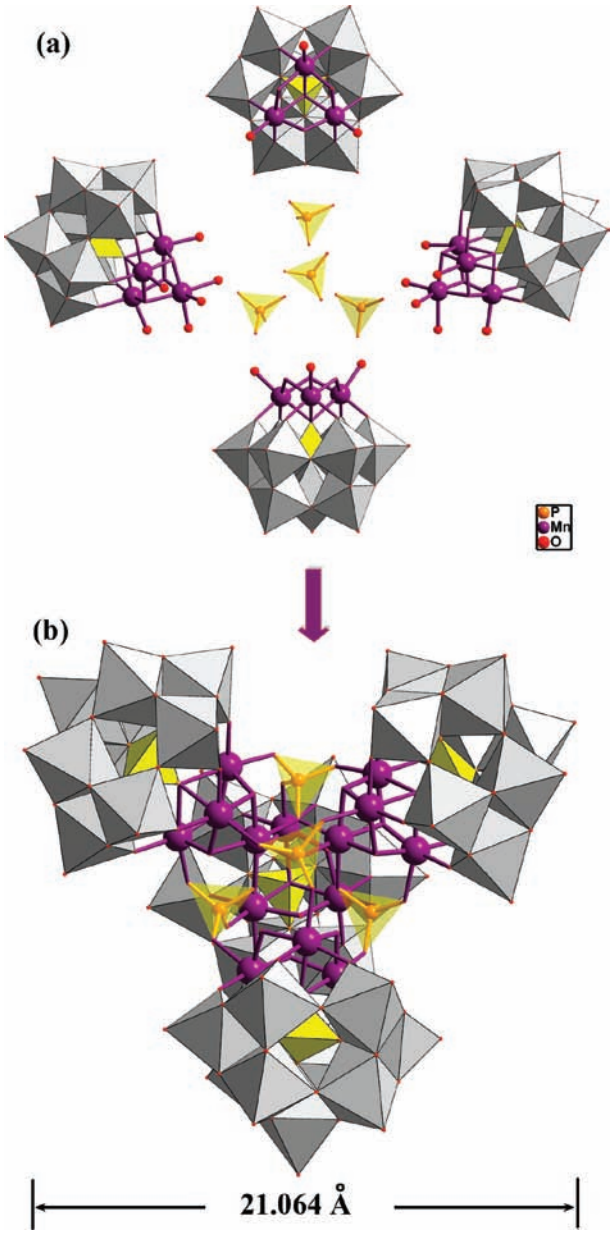

Figure 1. Polyhedral and ball-and-stick representations of (a) the basic building blocks and (b) their connection modes in the polyoxoanion of **1**.

coordination geometry. The bond lengths of P−O and the bond angles of O−P−O are in the ranges of 1.504(14)−1.572(11) Å and 107.6(7)−111.4(8)°, respectively. The bond lengths of W−O and bond angles of O−W−O vary from 1.655(15) to 2.514(14) Å and from 70.0(5) to 173.5(6)°, respectively (see Table S1 in the Supporting Information). In the $\{PW_9\}$ fragments, the trivacant sites are occupied by either $\{Mn_4\}$ cubelike complexes or $\{Mn_3\}$ triangular units. Furthermore, the four manganese-substituted $\{PW_9\}$ building blocks are fused by four $\{PO_4\}$ bridges to form the huge polyoxoanion of **1**. The largest diameter of the polyoxoanion is about 21.064 Å (as shown in Figure 1). In another point of view, if these $\{PW_9\}$ units were regarded as one kind of inorganic ligand, the polyoxoanion of **1** could also be described as a huge $\{Mn_{14}O_{12}(PO_4)_4\}$ complex wrapped by four $\{PW_9\}$ inorganic ligands.

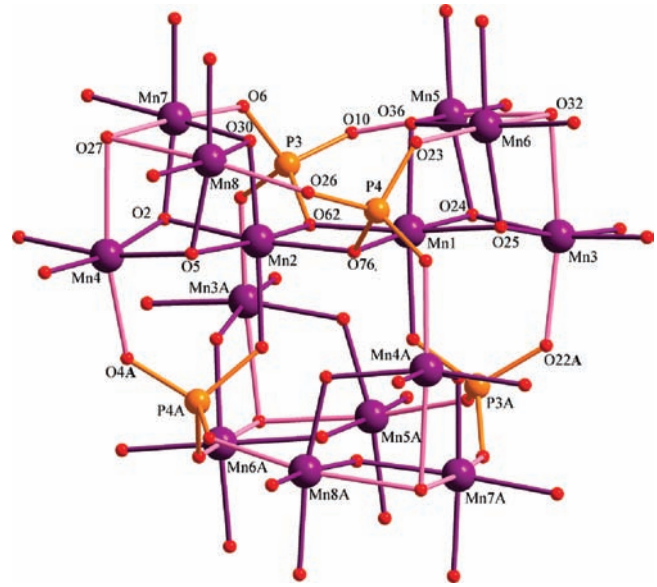

Figure 2. Ball-and-stick representation of the $[Mn^{III}_{13}Mn^{II}(\mu_2\text{-}O)_6(\mu_3\text{-}O)_6(\mu_4\text{-}PO_4)_2(\mu_5\text{-}PO_4)_2]$ core in **1**.

As shown in Figure 2, the central $\{Mn_{14}O_{12}(PO_4)_4\}$ aggregate consists of two $\{Mn_4\}$ cubelike complexes, two $\{Mn_3\}$ triangular complexes, and four $\{PO_4\}$ linkers. The two cubelike complexes are linked together via the Mn1−O76A−Mn2 and Mn1−O62A−Mn2 bridges, while the two triangular complexes are connected with $\{Mn_4\}$ moieties via the $\{PO_4\}$ bridges. In the $\{Mn_{14}O_{12}(PO_4)_4\}$ aggregate, all of the Mn atoms exhibit the distorted $\{MnO_6\}$ octahedral geometry; however, there are two types of coordination environments for the 14 manganese centers. A total of 12 Mn atoms (Mn3−Mn8 and their symmetry-related centers, Mn3A−Mn8A) are located in the trivacant positions of the $\{PW_9\}$ moieties and are coordinated with (i) two O atoms derived from the $[PW_9O_{34}]^{9-}$ anions, (ii) one O atom from the central $\{PO_4\}$ group of the POM moieties, (iii) one O atom from the bridging $\{PO_4\}$ unit, and finally (iv) two μ-/μ_3-O bridges. The Mn−O bond lengths and O−Mn−O bond angles are in the ranges of 1.886(13)−2.337(11) Å and 77.3(5)−174.3(5)°, respectively (see Tables 2 and S2 in the Supporting Information). Bond valence sum (BVS) calculations[19] indicate that all of these manganese centers exhibit a 3+ oxidation state (see Table S3 in the Supporting Information). A deeper analysis of these Mn−O bond distances shows that all of the Mn^{III} centers possess five short Mn−O bond distances [1.886(13)−2.112(14) Å] and a longer one [2.275(14)−2.334(14) Å]. Such an unusual structural feature of Mn^{III} is probably induced by the high rigidity of the POM skeleton and cannot show a clear Jahn−Teller effect. The other two Mn atoms (Mn1 and Mn2) are located in the central part of the huge aggregate, and they are coordinated with three O atoms derived from the $\{PO_4\}$ bridges and three μ_3-O bridges. The Mn−O bond lengths and O−Mn−O bond angles are in the ranges of 1.966(14)−2.339(14) Å and 81.0(6)−175.0(7)°, respectively. No obvious Jahn−Teller elongated axes (see Tables 2 and S2 in the Supporting

(19) Brown, I. D.; Altermatt, D. *Acta Crystallogr.* **1985**, *B41*, 244.

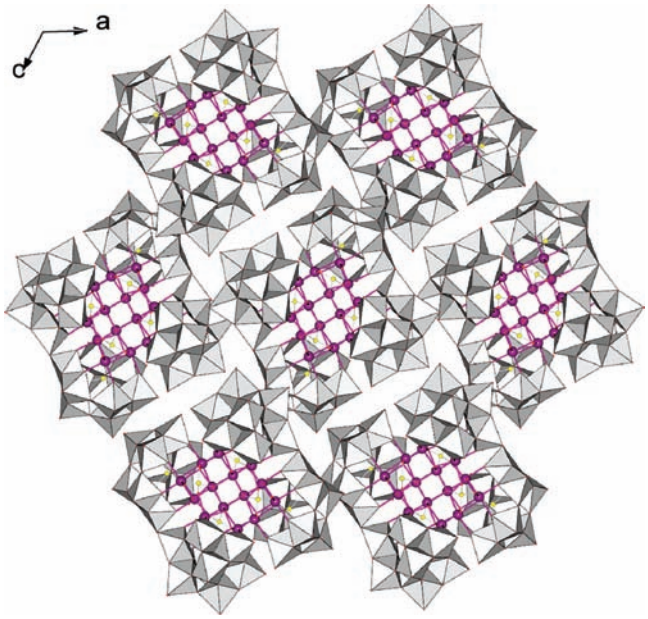

Figure 3. Packing arrangement of **1** viewed along the *b* axis. The cations and solvent water molecules are omitted for clarity.

Information) were observed for these two manganese centers (Mn1 and Mn2), and the BVS calculations show that both manganese centers exhibit a 2.5+ oxidation state (see Table S3 in the Supporting Information), suggesting that there should be one Mn^{2+} and one Mn^{3+} in these two Mn positions. In the $\{Mn_{14}O_{12}(PO_4)_4\}$ aggregate, the four $\{PO_4\}$ bridges exhibit different coordination abilities: two of them act as pentadentate ligands that can coordinate with five manganese centers; the other two just act as tetradentate ligands linked with four manganese centers (see Figure S3 in the Supporting Information). In addition, the 12 O bridges can also be separated into two groups: six of them act as μ_3-O bridges and link three manganese centers, while the other six O bridges act as μ-O bridges and connect two manganese centers (see Figure S3 in the Supporting Information). On the basis of the above analyses, the central aggregate can be described as a mixed-valent $\{Mn_{14}\}$ aggregate with the formula $[Mn^{III}_{13}Mn^{II}(\mu_2\text{-}O)_6(\mu_3\text{-}O)_6\ (\mu_4\text{-}PO_4)_2(\mu_5\text{-}PO_4)_2]$. To our knowledge, such a large mixed-valent $\{Mn_{14}\}$ aggregate represents so far the largest POM-based manganese aggregate in POM chemistry.

In the packing arrangement (see Figures 3 and S4 in the Supporting Information), all of the polyoxoanions are well separated and charged-balanced by the K^+ and Na^+ cations. Solvent water molecules are located in the interspaces between the large polyoxoanions, and they are hydrogen bonded with the surface O atoms of the POMs and/or coordinated with the countercations (K^+ and Na^+). It is worth mentioning that all of the $\{Mn_{14}O_{12}(PO_4)_4\}$ complexes are well wrapped and separated by the $\{PW_9\}$ moieties in **1**, allowing the magnetic core to be extremely well isolated from a magnetic point of view (i.e., interaggregate magnetic interactions are very unlikely).

IR, UV−vis, and XPS Spectra and TG Analysis. The IR spectrum of **1** (see Figure S5 in the Supporting Information) shows a broad peak at 3520 cm^{-1} and a strong peak at

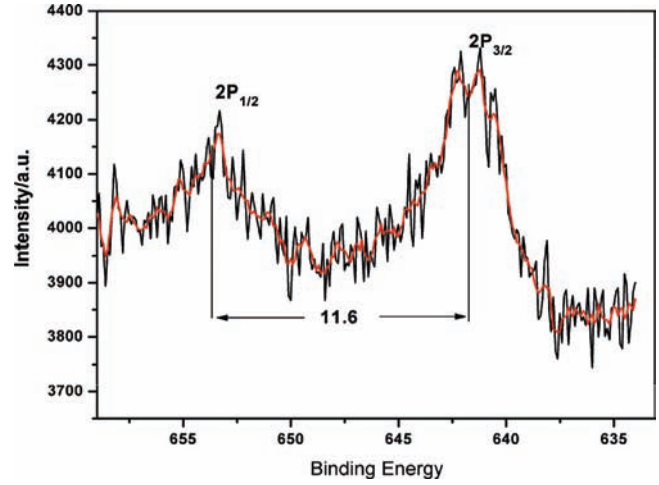

Figure 4. XPS spectrum of compound **1**

1620 cm^{-1} attributed to the lattice water molecules. The characteristic peaks at 1095, 970, 873, 732, and 615 cm^{-1} correspond to ν(P−O), ν(W=O_d), ν(W−O_b), and ν(W−O_c) vibrations, respectively.[9a] The UV−vis spectrum of **1** (see Figure S6 in the Supporting Information) displays two main peaks at 210 and 260 nm, which are attributable to the O → W ligand-to-metal charge-transfer bands.[9a] The broad bands in the visible region of 320−380 nm are mainly ascribed to the absorption of Mn^{3+} ions. TG analysis of **1** (see Figure S7 in the Supporting Information) exhibits two steps of weight loss. The first one of ca. 8.1% in the temperature range of 45−235 °C is attributed to the loss of all lattice water molecules. This value is consistent with the calculated value of 8.2% (~56 H_2O). The second weight loss of ca. 1.2% between 400 and 470 °C is probably the result of the loss of partial phosphorus oxide from the residue.

XPS was performed to identify the oxidation states of the manganese centers in compound **1**. As shown in Figure 4, the XPS spectrum of **1** exhibits one strong peak at 641.3 eV in the energy region of Mn $2p_{3/2}$ and one strong peak at 652.9 eV in the energy region of Mn $2p_{1/2}$. The distance between two main peaks is about 11.6 eV, which is consistent with the Mn^{3+} oxidation state.[20] It is noteworthy that BVS calculations suggest a Mn^{2+} center in compound **1**; however, the content of Mn^{2+} is very small, and its signal is probably overlapped by the Mn^{3+} centers.

Magnetic Properties. The magnetic properties of **1** were investigated on a polycrystalline sample. The temperature dependence of the magnetic susceptibility has been studied in the range of 1.8−300 K. As shown in Figure 5, the χT product at room temperature is 40.1 $cm^3 \cdot K \cdot mol^{-1}$, which is lower than the spin-only value ($g = 2.0$) of 43.375 $cm^3 \cdot K \cdot mol^{-1}$ for 13 noninteracting Mn^{III} ($S = 2$) ions and one Mn^{II} ($S = {}^5/_2$) ion. When the temperature was lowered, the χT product at 1000 Oe steadily decreased to reach a minimum of 4.9 $cm^3 \cdot K \cdot mol^{-1}$ at 1.8 K. This characteristic thermal behavior is indicative of dominant and strong

(20) (a) Han, Y.-F.; Chen, F.; Zhong, Z.; Ramesh, K.; Chen, L.; Widjaja, E. *J. Phys. Chem. B* **2006**, *110*, 24450. (b) Moro, F.; Corradini, V.; Evangelisti, M.; De Renzi, V.; Biagi, R.; del Pennino, U.; Milios, C. J.; Jones, L. F.; Brechin, E. K. *J. Phys. Chem. B* **2008**, *112*, 9729.

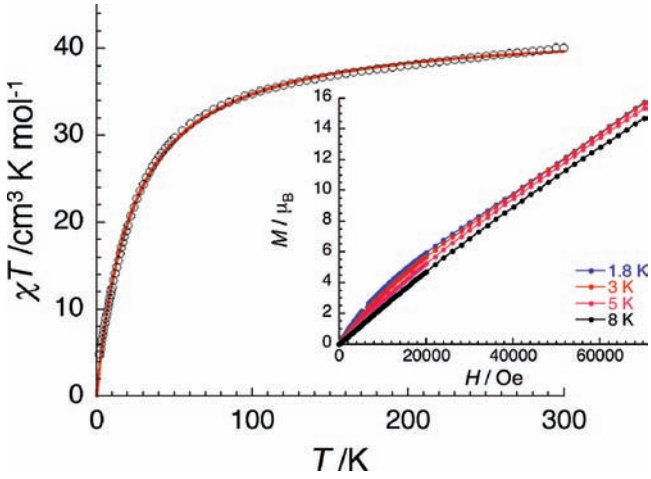

Figure 5. Temperature dependence of the χT product at 1000 Oe for **1** (with $\chi = M/H$ normalized per mole). The solid red line is the best fit of the experimental data with the Curie−Weiss law above 1.8 K. Inset: M vs H data at low temperatures for **1**.

antiferromagnetic interactions between manganese spins, which also explained the low χT product at room temperature. The experimental data have been well fitted by the Curie−Weiss law above 1.8 K with the following Curie and Weiss constants: 42.7(1) $cm^3 \cdot K \cdot mol^{-1}$ and −22.8(2) K, respectively (see Figure 5). The negative Weiss constant confirms the presence of dominating antiferromagnetic interactions between spin carriers, as was already mentioned above. Unfortunately, it was not possible to estimate the ground state of the $\{Mn_{14}\}$ units because no clear plateau is observed at low temperature on the χT vs T data. Furthermore, the field dependence of the magnetization has also been measured up to 7 T between 1.8 and 8 K (see the inset in Figure 5). It is worth noting that no hysteresis effect has been detected even at 1.8 K. The magnetic moment at 7 T and 1.8 K reaches 15.8 μ_B but is far from being saturated. Indeed, a linear field dependence is observed above 1 T, suggesting the progressive-field-induced population of the low-lying states of the $\{Mn_{14}\}$ core in **1**. This result indicates that, among the intramolecular antiferromagnetic interactions, some of them are small enough to be overcome by the applied dc field. It is worth mentioning that magnetic anisotropy induced by the presence of Mn^{III} metal ions is also minimally responsible for the M vs H behavior. In agreement with the absence of magnetic hysteresis at 1.8 K, no out-of-phase ac susceptibility (χ'') has been detected above 1.8 K.

In conclusion, a new $\{Mn_{14}\}$ aggregate based on the inorganic POM ligands has been successfully prepared via the reaction between the lacunary polyoxoanion $[PW_9O_{34}]^{9-}$ and the $[Mn_{12}(CH_3COO)_{16}(H_2O)_4O_{12}]$ complex. Compound **1** represents the largest manganese aggregate based on inorganic POM ligands. Moreover, the synthesis of **1** suggests a new route for the preparation of POM-based high-valent manganese complexes. The magnetic investigation shows that compound **1** exhibits strong antiferromagnetic interactions in the inner $\{Mn_{14}\}$ cores. Further research will focus on the reactions between various other lacunary POM ligands and the $\{Mn_{12}\}$ complex in order to obtain new types of POM-based mixed-valent manganese complexes with interesting magnetic properties.

Acknowledgment. This work was supported by the National Natural Science Foundation of China (Grant 20701005), the Postdoctoral station Foundation of the Ministry of Education (Grant 20060200002), the Science and Technology Creation Foundation of Northeast Normal Univerisity (Grant NENU-STC07009), the European network MAGMANet (Grant NMP3-CT-2005-515767), the University of Bordeaux, the CNRS, and the Région Aquitaine. We also thank E. Harté for technical support on the SQUID magnetometer.

Supporting Information Available: ORTEP diagrams of **1** and **2**, possible core ararangements, packing arrangement, coordination environments, IR and UV−vis spectra, TG analysis, bond lengths and angles, and BVS calculations. This material is available free of charge via the Internet at http://pubs.acs.org.

IC802023H